Journal of Engineering, Project, and Production Management
2026, 16(1), 2025-170

Population Aging Urban Scheduling Management Algorithm Combining Cluster Decomposition and Improved Hybrid Ant Colony Algorithms

Fei Pang[1], Yingxu Li[2], Guo Miao[3], and Yun Shi[4]
[1] Associate Professor, School of Education Science, Hanshan Normal University, Chaozhou, 52041, China
[2] Associate Professor, College of Economics Management, Hanshan Normal University, Chaozhou 52041, China
[3] Associate Professor, Regional Modernization Institute, Jiangsu Academy of Social Sciences, Nanjing 210046, China
[4] Lecturer, School of Education Science, Hanshan Normal University, Chaozhou 52041, China, E-mail: YunShiys@outlook.com (corresponding author).

Project Management
Received August 20, 2025; revised September 29, 2025; accepted October 6, 2025
Available online December 14, 2025

Abstract: The aging population is intensifying spatiotemporal imbalances in the supply and demand of urban medical and transportation resources. Traditional static planning algorithms need to adapt to the dynamic, clustered nature of demand from elderly residents. To address the limitations of experience-dependent, non-driven traditional scheduling, this paper proposes a novel urban management algorithm that integrates clustering decomposition with an improved hybrid Ant Colony Optimization (ACO) technique. The proposed framework employs a two-layer clustering model. The first layer utilizes an adaptive K-means++ algorithm to optimize the placement of elderly care service base stations by integrating demand intensity and spatial accessibility. The second layer applies a K-medoids algorithm with a walking distance matrix to achieve balanced task allocation. Building on this structure, we designed an enhanced ant colony optimization algorithm, incorporating a genetic algorithm to solve the shortest-path problem with time windows. Key improvements include adaptive initial pheromone generation, a dynamic volatilization mechanism, and a local search strategy. Experimental results in 20×20 and 30×30 grid scenarios demonstrate that our framework shortens path lengths by 18.0% and increases convergence speed by 140% compared with the traditional Ant Colony Optimization. Taking Shanghai's aging community as an example, the model reduced average response time by 25%, increased resource coverage efficiency by 30%, and significantly improved personal load balancing. This research offers a solution that both combines theoretical innovation and practical value for efficient resource allocation in cities with aging populations.

Keywords: Ant colony algorithm, K-means++, cluster decomposition, population aging, scheduling management.

DOI 10.32738/JEPPM-2025-170

1. Introduction

Population aging has become a core challenge for global socio-economic development in the 21st century. According to the United Nations' 2023 World Population Prospects report, the global population ages 65 and above is projected to reach 16% by 2050, with this trend being more pronounced in emerging economies like China (Shou et al., 2024; Sarker et al., 2023). This demographic shift intensifies spatiotemporal imbalances in the supply and demand of core urban resources such as healthcare, transportation and community services. For instance, elderly medical demands exhibit distinct “morning peak” and “community concentration” clustering patterns, while their activities impose stricter requirements on public transit accessibility. This challenge can be framed as a complex urban resource scheduling problem: how to optimize the placement of service-based stations and plan efficient service personnel routes to cover all demand points within a dynamically changing environment. However, existing research often relies on static linear programming or a single heuristic algorithm, which have significant limitations in aging-population scenarios (Dural Selcuk and Vasilakis, 2023; Mpia et al., 2025). For example, classical Genetic Algorithms (GA) often converge on local optima with multiple constraints, and cannot effectively integrate real-time demand data. Although rule-based expert systems can handle priority logic, they lack the flexibility to adapt to sudden events, such as regional disease outbreaks among the elderly (Klose et al., 2023; Li et al., 2024). A more fundamental issue is that most algorithms fail to fully account for the spatiotemporal clustering characteristics of aging-related demand. For instance, medical service requests often cluster during morning rush

hours and within specific communities. The fixed parameter settings of traditional ACO algorithms are ill-suited to these dynamic conditions (Saranya and Karthik, 2024).

Li et al. (2023) proposed a decomposition and ensemble clustering to extract wide interference fringes from underwater sonar signals, a traditionally challenging task. Their approach decomposes the spectrogram into background, stripes, and noise components, applying a multi-phase ensemble clustering algorithm to identify parabolic features. Experiments on both simulated and real datasets demonstrate that this method effectively extracts stripes with performance comparable to the Hough transform. To overcome the sensitivity of traditional clustering algorithms to data dimensionality and cluster count, Moghadam and Ahmadi (2024) introduced a two-stage biomimetic method based on the stage algorithm, which combines partitioning with an improved search strategy. Experiments on six real and three generated datasets showed it outperformed eight traditional methods across multiple clustering metrics and exhibited superior adaptability to high-dimensional data. Chen et al. (2024) addressed feature interference, similarity, and feature selection issues in time-series deep clustering by proposing a two-stage multi-view method using a one-dimensional deep convolutional auto-encoder. Multi-scenario verification confirmed that this approach significantly outperformed traditional methods such as K-means, hierarchical clustering, and deep learning methods in terms of accuracy and spatial linear separability. In transportation, Chen et al. (2025) proposed a two-stage flow clustering method integrating Leiden community detection with shared-nearest-neighbor to analyze shared bicycle mobility patterns. Their results revealed that 71.85% of morning and 65.79% of evening rush-hour flow clusters served subway connectivity demand, providing a decision-making basis for allocating transportation resources. Finally, Yastrebov et al. (2023) created a fuzzy cognitive map modeling technique that combines k-means clustering with a multi-objective evolutionary algorithm for diabetes medical data. Their experiments indicate that models built from grouped data achieved higher predictive accuracy than standard methods, suggesting new avenues for personalized medicine.

Fan (2024) proposed a two-stage hybrid ACO for the time-varying electric vehicle routing problem in multi-warehouse semi-open environments. This algorithm enhanced K-means clustering for customer allocation and an improved ACO for routing. Simulation results showed that it effectively reduced both carbon emissions and logistics costs, contributing to the sustainable development of urban logistics. Mulo et al. (2023) developed a hybrid acoustic search optimization method for economic dispatch of power grids with renewable energy. Experiments in a 26-bus system demonstrated its ability to handle wind energy uncertainty, reduce power generation costs, and provide viable solutions for clean energy grid integration. Wenya and Ze (2025) constructed a multi-objective optimization model for cross-border logistics of biotechnology products, solved with an improved ACO. This experiment achieved a path planning accuracy of 94.39%, providing an efficient solution for cross-border e-commerce. Wang et al. (2025) proposed an urban solid waste management model based on an improved ACO algorithm. The model introduced asynchronous constraints in a connected vehicle environment to alleviate congestion and a combined collection and transportation system for waste classification. Compared to separate and unified schemes, it reduced costs by 5.38% and 2.75%, respectively. Yu (2024) designed a path planning model using an improved ACO algorithm, which incorporated a rollback strategy to optimize the taboo table and integrated an enhanced A* algorithm for global path planning and dynamic obstacle avoidance. Simulation experiments showed the model reduced the average search time by 4.11% and the average path length by 22.07% in complex environments, providing an efficient method for urban green traffic management.

In summary, most studies rely on static programming models or preset parameters, such as traditional K-means or basic ACO algorithms, which fail to effectively capture and adapt to spatiotemporal fluctuations in the aging population's demands. When handling multi-objective, multi-constraint scheduling problems, single heuristic algorithms often suffer from premature convergence or local optima, while existing hybrid strategies tend to focus solely on algorithmic improvements without deep integration of the problem's inherent data characteristics. Furthermore, prevailing urban scheduling research frequently treats service demand points as independent or evenly distributed, to resource allocation and task assignment schemes that deviate and fail to achieve true load balancing and efficient response. To address these three core limitations, the existing research on the scheduling of aging cities, namely the difficulty of static models in adapting to dynamic demands, the difficulty of a single algorithm in handling complex constraints, and the neglect of the spatio-temporal clustering characteristics of demands, this paper proposes a scheduling management algorithm for aging populations that combines clustering decomposition and an improved hybrid ACO. The core innovation of this algorithm lies in transforming the complex macroscopic scheduling problem into structured sub-problems through a two-layer clustering model, then using the improved GA-ACO hybrid algorithm to efficiently solve each sub-problem, ultimately achieving full-process optimization from resource layout to path execution.

The novel contributions of this paper are threefold: (1) We propose an adaptive K-means++ algorithm for spatiotemporal clustering that introduces a dynamic weight mechanism based on real-time demand intensity and spatial accessibility, along with dynamic constraint strategies during integration. This overcomes key limitations of traditional clustering, sensitive to the initial centroids and an inability to adapt to dynamic demands, enabling a scientific layout for elderly care service stations. (2) A hybrid ACO enhanced by a genetic algorithm was designed, which innovatively uses the GA's search capability to generate a high-quality initial pheromone distribution for the ACO. This effectively balances global exploration with local development capabilities, accelerating convergence and avoiding premature stagnation. (3) We constructed an integrated "clustering decomposition-path-optimization" framework that systematically addresses the full-process optimization concerns from macro resource allocation to micro path execution, with demonstrated superiority in both simulation and real-world case studies.

2. Methods and Materials

This paper proposes a collaborative framework that integrates a two-layer clustering decomposition model with an

improved hybrid ACO. The framework employs an adaptive K-means++ algorithm to optimize service base station layouts and a Walking Distance Matrix K-medoids Algorithm (WDM-KM) algorithm used to achieve balanced task allocation. These are combined with a GA and enhanced ACO strategy to solve the shortest service path. Ultimately, this constructs a comprehensive algorithm system for scheduling and management in aging cities.

2.1. Service Demand Clustering Model Based on Spatial Characteristics

With the intensification of population aging, demand for urban elderly care services exhibits significant spatial clustering and dynamic fluctuations, making traditional static layout models inadequate for aging cities. Therefore, a multi-level clustering model that integrates spatial geographic coordinates, demand intensity, and facility accessibility is proposed. Aging service demands are accurately clustered through adaptive weighting mechanisms and dynamic constraint strategies. The proposed algorithmic framework for urban scheduling is shown in Fig. 1. The overall architecture is designed as a progressive two-layer clustering framework, which gradually reduces and aggregates the large-scale, while high-dimensional urban elderly care service demand is set through a step-by-step and layered strategy, transforming it into a manageable and operable scheduling unit. This model first decomposes the city-level scheduling problem into multiple manageable sub-regions through dimensionality reduction and simplification, while also enabling professional division of labor. The first layer focuses on the spatial location optimization of service base stations, while the second layer is dedicated to the balanced distribution of the workload of service personnel, enabling each layer's algorithm to specifically address core contradictions. Ultimately, this ensures that tasks allocated to each service employee are spatially compact and balanced in workload, while guaranteeing overall path efficiency from the outset.

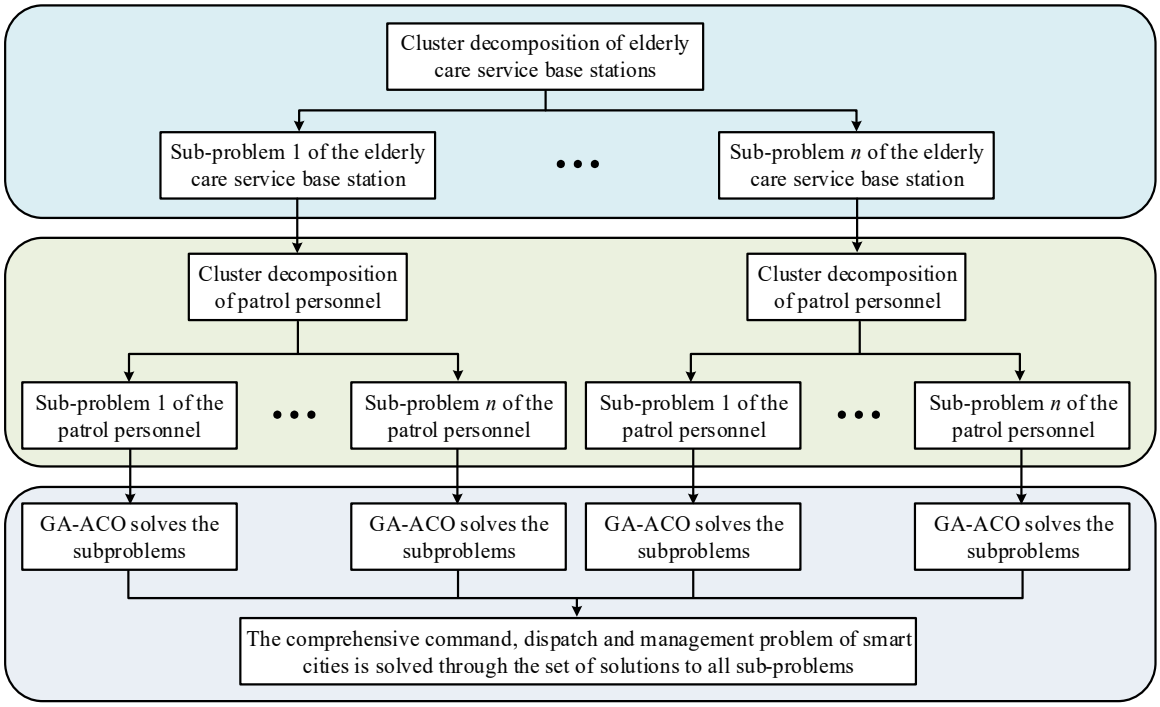

Fig. 1. Framework of the dispatching and management algorithm for cities with an aging population

The first layer of clustering focuses on optimizing location selection for service base stations. Its core objective is to determine a set of elderly care service base stations with optimal spatial locations while satisfying coverage constraints and capacity limitations, so as to minimize the total cost of spatial accessibility from all demand points to their respective base stations. The standard K-means++ algorithm is extremely sensitive to initial cluster centers and is prone to getting stuck in local optima. However, the K-means++ algorithm improves the quality of initial solutions and robustness of the algorithm through a distance probability based initial center point selection strategy (Gao et al., 2023; Bai et al., 2023). Therefore, the K-means++ algorithm is chosen for the study, and an adaptive weight mechanism is further introduced to improve the algorithm. During the iteration process, the influence weight ω_i of each demand point on the cluster center position is no longer fixed, but can be adjusted based on the real-time demand intensity D_i of that point and the spatial constraints of the current state.

Demand intensity D_i usually refers to the amount of elderly care services required at a specific point in time, such as service duration, frequency, or resource quantity. It is a key indicator reflecting the urgency and importance of demand. The objective function J is defined as the minimization of the weighted sum of squared distances, as shown in Eq. (1).

$$J = \sum_{k=1}^{K} \sum_{i \subset C_k} \omega_i \cdot \|x_i - c_k\|^2 \tag{1}$$

In Eq. (1), K represents the total number of elderly care service base stations (cluster centers) that need to be determined, which is pre-set according to the actual situation. C_k is the set of all demand points allocated to the k -th base station. $x_i = (x_i, y_i)$ represents the two-dimensional geographic coordinate vector of the i -th demand point. $c_k = (c_{kx}, c_{ky})$ represents the two-dimensional geographic spatial coordinate vector of the k -th elderly care service base station. $\|x_i - c_k\|$ represents

the Euclidean distance, which is usually used to calculate the straight-line spatial distance from the demand point i to the base station k. ω_i assigns dynamic weights to the i -th demand point. It is calculated through the demand intensity D_i and spatial accessibility factor A_i, as shown in Eq. (2).

$$\omega_i = f(D_i, A_i) = \alpha \cdot \frac{D_i}{D_{max}\frac{A_i}{A_{max}}} \tag{2}$$

In Eq. (2), D_{max} and A_{max} are the maximum values of demand intensity and accessibility factors among all demand points, respectively, used for normalization processing. α and β are proportional coefficients for adjusting weight allocation, satisfying $\alpha + \beta = 1$, which is used to balance the relative importance of demand intensity and spatial accessibility in base station site selection. This dynamic constraint strategy is reflected in the algorithm iteration process, which checks and ensures in real-time that each initially formed cluster meets the preset constraint conditions. The dynamic constraint strategy is shown in Eq. (3).

$$\begin{aligned} &Constraint\ 1\text{: } \max_{i \subset C_k} \| \boldsymbol{x}_i - \boldsymbol{c}_k \| \leq R_{max} \\ &Constraint\ 2\text{: } \sum_{i \subset C_k}^{\Sigma} D_i \leq C_{max} \end{aligned} \tag{3}$$

In Eq. (3), R_{max} is the maximum service radius within the cluster. C_{max} is the maximum service capacity of a single base station. If the clusters generated by iteration violate constraints, the center point adjustment or demand point reallocation mechanism will be triggered (Chowdhury et al., 2024; Zhang et al., 2024). The process of the adaptive K-means++ algorithm is shown in Fig. 2. This process iteratively selects the initial center, assigns clusters and updates centroids, traverses a preset number of intervals, and finally outputs a set of optimized geographic coordinates $\{c_1, c_2, \ldots, c_K\}$ of elderly care service base stations, as well as the base station identification k_i to which each demand point i belongs.

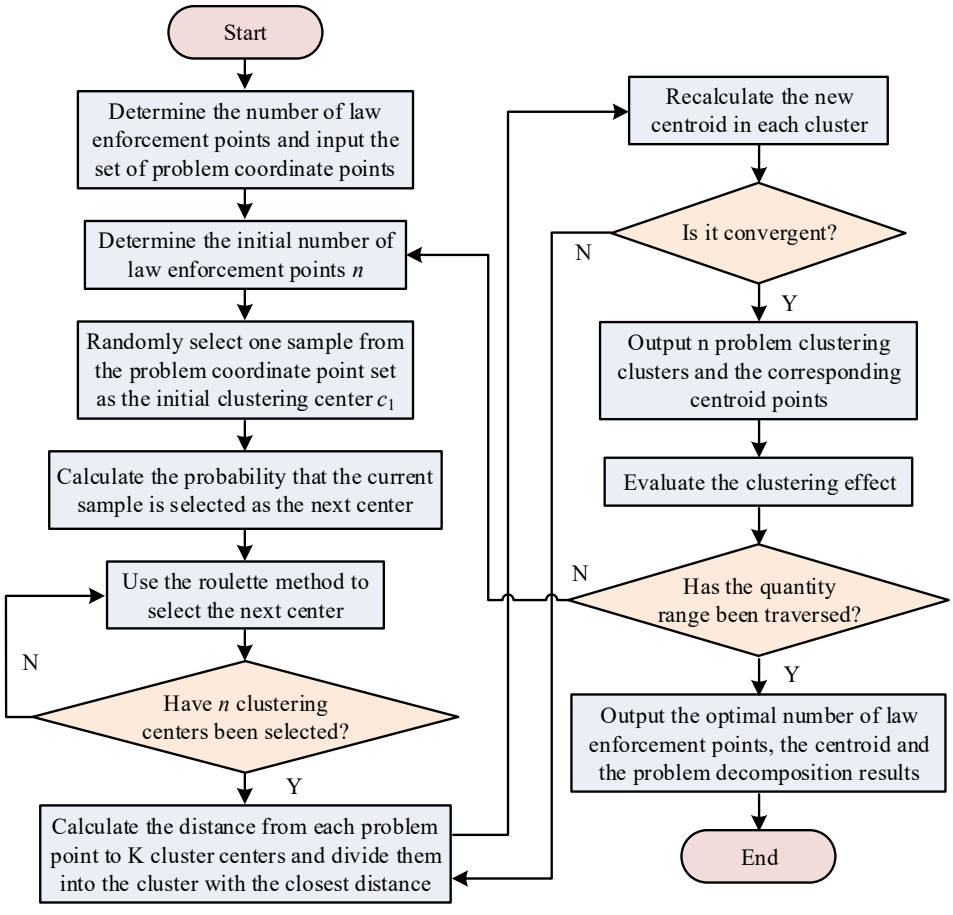

Fig. 2. The process of the adaptive K-means++ algorithm

To quantify clustering quality, the Silhouette Coefficient (SC) and the Davies-Bouldin Index (DBI) are introduced as evaluation indicators. SC measures the intra-cluster cohesion and inter-cluster separation. DBI measures the similarity between clusters. The calculation is shown in Eq. (4).

$$\begin{cases} SC = \frac{1}{N}\sum_{i=1}^{N} \frac{b_i - a_i}{max(a_i, b_i)} \\ DBI = \frac{1}{N}\sum_{i,j=1}^{N} \max_{i \neq j}\left(\frac{s_i + s_j}{d_{i,j}}\right) \end{cases} \tag{4}$$

In Eq. (4), a_i is the average distance from point i to other points within the same cluster, which reflects the degree of

clustering within that cluster. b_i is the average distance from point i to the nearest neighboring cluster, reflecting the degree of separation between clusters. s_i and s_j are the average distances from all sample points within the i -th and j -th clusters to the cluster center. $d_{i,j}$ is the center distance between clusters.

The second layer of clustering is carried out within the service coverage area of the base station formed in the first layer. Its core task is to further divide all demand points assigned to the same base station into several finer sub-clusters. Each sub-cluster will ultimately be responsible for responding to all internal service requirements by service personnel. Therefore, the clustering results of this layer directly determine the specific task allocation plan for service personnel. This layer adopts the WDM-KM algorithm. For the demand point set C_k assigned to a specific base station k, the dissimilarity between its internal points i and j is defined as the walking distance between them, as shown in Eq. (5).

$$\text{dissim}(i,j) = d_{ij}^{(walk)} \tag{5}$$

The objective function J_k is to find P_k Medoids and allocate non-Medoid points to the nearest Medoid point, so as to minimize the total walking distance between all non-Medoid points and their corresponding Medoid points, as shown in Eq. (6) (Ranjbar Noshari et al., 2024; Zheng et al., 2023).

$$J_k = \sum_{m=1}^{P_k} \sum_{i \in S_m} d_{i,m_i}^{(walk)} \tag{6}$$

In Eq. (6), P_k is the number of service personnel allocated to the base station. S_m is the set of demand points assigned to the m -th service personnel. $d_{i,m_i}^{(walk)}$ represents the walking distance from the demand point i to its corresponding Medoid point. m_i is an actual demand point in C_k, representing the task distribution center of the m -th service personnel. This layer also needs to incorporate dynamic constraint strategies, with the most important constraint being to ensure that the total demand intensity $\sum_{i \subset S_m} D_i$ of all demand points allocated to each service personnel m does not exceed their service capacity upper limit $L_{\max}$. The maximum walking distance between any two points within the cluster is controlled within a reasonable service response time, as shown in Eq. (7).

$$\begin{aligned} &Constraint\ 3: \sum_{i \subset S_m} D_i \le L_{max}, \quad \forall m \in \{1,2,\ldots,P_k\} \\ &Constraint\ 4: \max_{i \subset S_m} d_{i,m_i}^{(walk)} \le T_{max}, \quad \forall m \in \{1,2,\ldots,P_k\} \end{aligned} \tag{7}$$

The process of WDM-KM algorithm is shown in Fig. 3. Firstly, select P_k initial Medoid points are selected randomly or based on distance in C_k. Then, each non-Medoid point in C_k is assigned to the Medoid point with the closest walking distance, forming a temporary sub-cluster $\{S_1, S_2, \ldots, S_{P_k}\}$. The point that minimizes the total distance change is taken as the new Medoid. If the current partition satisfies Eq. (7) is checked. If violated, the sub-cluster partitioning needs to be adjusted. The allocation phase and update phase are repeated until the Medoid point no longer changes or reaches the maximum iteration count, and all constraints are satisfied.

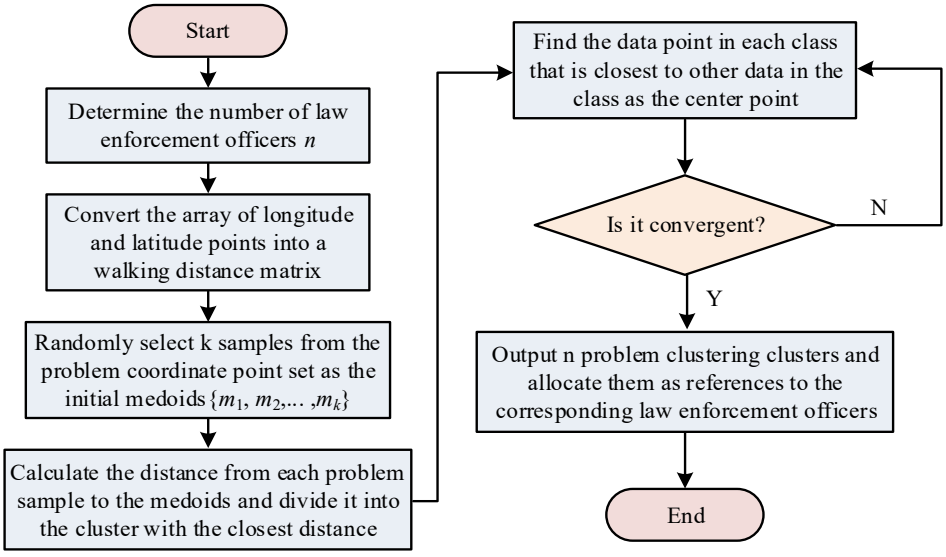

Fig. 3. The process of the WDM-KM algorithm

2.2. Design of Improved Hybrid Ant Colony Algorithm

Through the two-layer clustering decomposition in the previous stage, the original large-scale scheduling problem is decomposed into $N \times K$ single nursing staff sub-problems. Each sub-problem can be described as: Given a law enforcement officer and a set of service demand points to be inspected, a shortest path that efficiently covers all points while satisfying constraints such as time windows and physical exertion is planned. The essence of this problem is a

constrained vehicle routing problem, which belongs to the NP-Hard problem. To improve the efficiency and quality of problem-solving, an improved hybrid ACO is taken for problem solving. The core process is shown in Fig. 4. This algorithm combines the global search capability of GA with the local optimization capability of ACO, and generates initial pheromone distributions through GA to improve the convergence speed and solution quality of ACO.

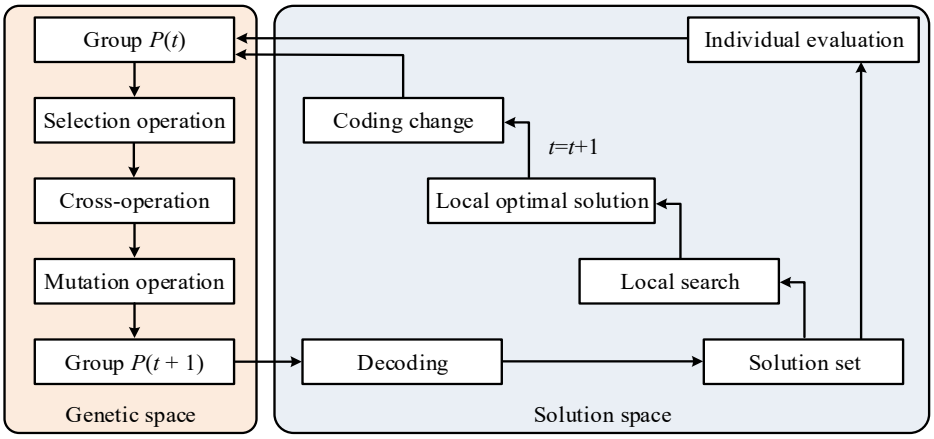

Fig. 4. Schematic diagram of the composition of the hybrid genetic algorithm

In the initialization stage of pheromones, a feasible path consisting of P randomly generated based on simple heuristic rules (such as the nearest neighbor method) is initialized to form the initial population P of the GA, providing a high-quality gene library for subsequent genetic operations. In the t -generation of algorithm iteration, each ant m starts from the service base station v_0 and gradually constructs a closed service path covering all S service demand points and ultimately returning v_0 based on a state transition rule. When ant q is currently located at vertex i, the probability $p_{ij}^q(t)$ of its next choice to move to unvisited vertex j is determined by the pheromone concentration $\tau_{ij}(t)$ and heuristic information η_{ij}. The specific calculation follows the random proportion rule, as shown in Eq. (8).

$$p_{ij}^q(t) = \begin{cases} \frac{[\tau_{ij}(t)]^\alpha \cdot [\eta_{ij}]^\beta}{\sum_{k \in \text{allowed}_q} [\tau_{ik}(t)]^\alpha \cdot [\eta_{ik}]^\beta} & \text{if } j \in \text{allowed}_q \\ 0 & \text{otherwise} \end{cases} \tag{8}$$

In Eq. (8), α is the pheromone heuristic factor, which regulates the importance of pheromone accumulation. The larger the value, the more ants tend to choose the path that they have passed through more times before (pheromone rich). β is the expected heuristic factor, which regulates the importance of heuristic information. The larger the value, the more ants tend to choose the next vertex that is closer in distance, allowing d_q to represent the set of service demand points that Ant q is allowed to access in its current state, but has not yet reached. This process continues until Ant q has accessed all S service demand points and finally returns to service base station v_0. The total length of the path $L^q(t)$ is calculated as its cost.

After all M ants complete the path construction in each iteration. The algorithm does not immediately update the pheromone, but first performs the GA operation, using the path information explored by the ant colony to generate a new optimized solution set. Firstly, the fitness $F^q(t)$ of each path in the current ant population is calculated, as shown in Eq. (9).

$$F^q(t) = \frac{1}{L^q(t) + \lambda \cdot max(0, Seg^q - d_{max}} \tag{9}$$

In Eq. (9), Seg^q represents the length of the longest uninterrupted patrol sub-path in the path. λ is the penalty coefficient. Based on fitness values, the roulette wheel selection method is used to select p optimal paths from the paths of M ants as parent individuals, as shown in Eq. (10).

$$p_s^q = \frac{F^q(t)}{\sum_{r=1}^{M} F^r(t)} \tag{10}$$

In Eq. (10), p_s^q represents the probability of the q -th path being selected. In the crossover operation of path sequences, an improved partial mapping crossover strategy is adopted for special structures containing fixed law service base stations. The operation process is shown in Fig. 5.

According to Fig. 5, first, identify and record the parent path sequence and the location of the intermediate law service base station. Subsequently, remove the service base stations from the sequence and only retain the sequence of service demand points that need to be inspected. On the remaining sequence of service demand points, randomly select two tangent points and swap the sub-sequence segments between these two tangent points. Next, based on the mapping relationship established by the exchanged fragments, the duplicate service demand points that appear in the exchanged sequence are transformed to ensure the legitimacy of the sequence. Finally, reinsert the previously recorded service base stations into their original positions to generate two new offspring path sequences. The mutation operation is used to introduce random perturbations into the population to prevent premature convergence of the algorithm. The operation process is shown in Fig. 6.

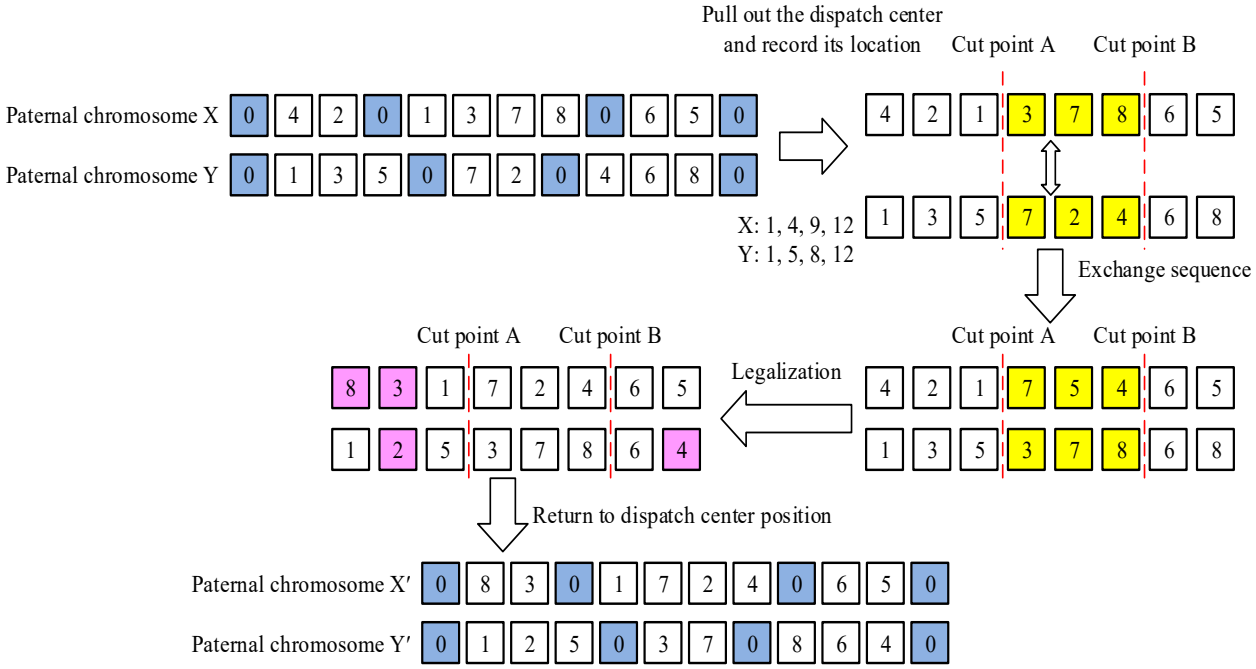

Fig. 5. Improved partial mapping crossover strategy

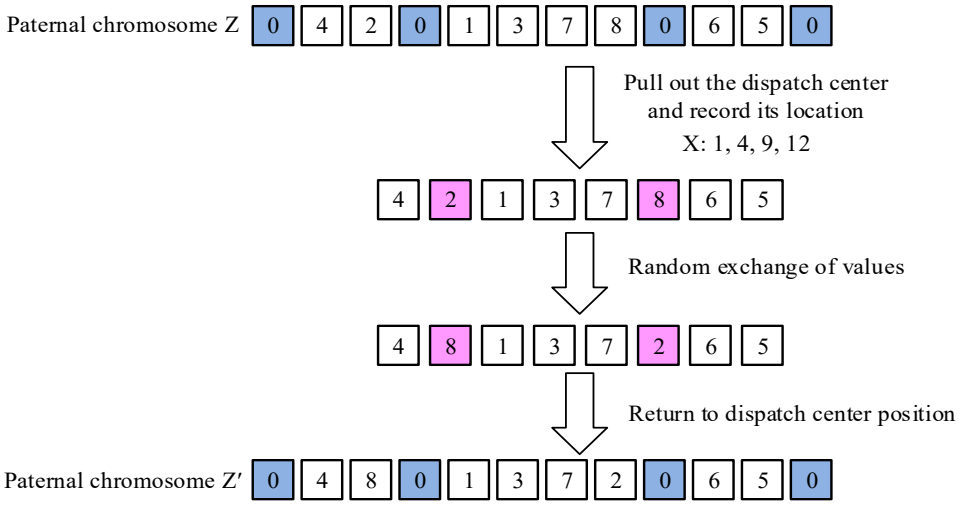

Fig. 6. Mutation operation

In Fig. 6, first, identify and record the position of the service base station in the sequence of paths to be mutated, and remove it. Randomly select two positions in the remaining sequence of service demand points and swap the order of service demand points at these two positions. Subsequently, reinsert the law service base station into its original position to generate a new path sequence. Compared to other mutation operators, swapping mutations can introduce changes while maintaining the rationality of the path structure (Tanimu et al., 2024; Jasim and Kurnaz, 2024). The mathematical expression of the exchange mutation operation is Eq. (11).

$$\pi_{\text{new}}[i] \leftrightarrow \pi_{\text{new}}[j] \quad \text{where} \quad i, j \sim u\{1,2,\dots,S\}, \quad i \neq j \tag{11}$$

In Eq. (11), π_{new} represents the sequence of paths to be mutated. u represents a discrete uniform distribution. Updating pheromones involves two steps. Firstly, the volatility of pheromones is simulated to mimic the natural dissipation process of pheromones in nature to prevent the infinite accumulation of pheromones from causing algorithm stagnation (Xu et al., 2024). All pheromones on edge (i, j) decrease according to the rule shown in Eq. (12).

$$\tau_{ij}(t) \leftarrow (1-\rho) \cdot \tau_{ij}(t) \tag{12}$$

In Eq. (12), ρ is the volatility coefficient of pheromones. Not all ants or genetic individuals release pheromones, but only the contemporary optimal ant path τ_{ij}^{bs} or the optimal individual path τ_{ij}^{gb} generated by genetic manipulation is allowed to release pheromones to enhance learning of high-quality paths (Stodola and Nohel, 2022). The rule for pheromone

enhancement is shown in Eq. (13).

$$\tau_{ij}(t+1) = \tau_{ij}(t) + \Delta\tau_{ij}^{bs} + \Delta\tau_{ij}^{gb} \tag{13}$$

To prevent premature convergence caused by extreme differentiation of pheromone concentration, a pheromone boundary restriction mechanism is introduced, as shown in Eq. (14).

$$\tau_{ij}(t+1) \leftarrow min(\tau\, max(\tau ij_{min}())_{max}) \tag{14}$$

In Eq. (14), τ_{max} and τ_{min} are the preset lower and upper limits of pheromone concentration, respectively. This elite strategy can significantly accelerate algorithm convergence to high-quality solutions (Theodorou and Christopoulos, 2024). To further balance the exploration and development capabilities of the algorithm and enhance its robustness in multi-constraint scenarios in aging cities, the pheromone volatilization coefficient ρ adopts an adaptive mechanism, as shown in Eq. (15).

$$\rho(t) = \rho \frac{t}{T_{max}} minmax_{min} \tag{15}$$

In Eq. (15), ρ_{min} and ρ_{max} are the preset minimum and maximum volatility coefficients. In the initial stage of the algorithm, $\rho(t)$ is relatively small, which is conducive to preserving diversity for extensive exploration. As the iteration progresses, an increase in $\rho(t)$ prompts the algorithm to concentrate pheromones on the most promising path in the later stages, strengthening its development capabilities (Wu et al., 2024; He et al., 2024).

When the termination condition is met, the algorithm outputs the global optimal service path and its length corresponding to the sub-problem of the nursing staff. The GA-ACO hybrid framework utilizes parallel path construction and positive feedback mechanism of ACO to quickly discover optimal solution regions, and then uses selection, crossover, and mutation operations to conduct deep mining and jump out of local optima on a global scale. The elite pheromone update strategy ensures the effective accumulation and transmission with the use of high-quality solution information.

3. Results

To quantify the effectiveness of the proposed model, a simulated experimental environment is built with 20×20 and 30×30 grid scenarios, combined with real cases of medical service scheduling in aging communities in Shanghai. The validation is carried out from multiple dimensions such as clustering quality, path optimization efficiency, and response time.

3.1. Simulation Experiment and Algorithm Performance Verification

The experimental environment is set up on a desktop computer configured with an Intel Core i7-12700K processor (3.6GHz, 12 cores), 32GB DDR4 memory, NVIDIA GeForce RTX 3060 graphics card, and Ubuntu 20.04 LTS operating system. The algorithm implementation is based on Python 3.8, mainly relying on Scikit-learn 1.0.2 to complete clustering analysis, using Matplotlib 3.5.3 for visualization, and building a simulation grid through Pygame 2.1.2. The path plan utilizes the ANTsPyOpt 1.1.0 library to optimize the ACO parameters. The convergence curve of the algorithm is monitored through TensorBoard 2.9.1 during the experimental process.

Table 1. Parameter settings of GA-ACO algorithm

Parameters	Symbol	Value
Initial pheromone	τ	0.2
Population size	P	80
Cross probability	-	0.8
Mutation probability	-	0.05
The maximum number of iterations of the genetic algorithm	-	45
The number of ants	M	60
Pheromone weight control coefficient	α	3
Visibility weight control coefficient	β	2
Volatilization coefficient	ρ	0.3
Pheromone increases the intensity coefficient	-	10
The number of converges of ant colony algorithm	-	3

The dataset is constructed using a mixed-mode approach. One is a publicly available dataset, referencing the distribution data of the population ages 65 and above from the United Nations' World Population Prospects 2023 (Website: https://population.un.org/wpp/) and OpenStreetMap (OSM) Shanghai Pu District Road Network Data (Website: https://www.openstreetmap.org/), the elderly population density (unit: person/km^2) and road connectivity matrix (including 500+nodes) from Jing'an, Huangpu, Chongming, Jinshan and other areas are extracted. The second is a simulated dataset, which randomly generates 20×20 and 30×30 grid scenarios using Python. Each grid cell corresponds to a virtual community, including the number of elderly population (randomly distributed between 10-50 people), service request time (following the normal distribution of morning peak), and walking distance constraints. The 20×20 grid contains 400 community nodes, and the 30×30 grid expands to 900 nodes for simulating large-scale scheduling scenarios. All data are normalized using Z-Score to ensure consistency in the input dimensions of the algorithm. The GA-ACO algorithm parameter settings are shown in Table 1.

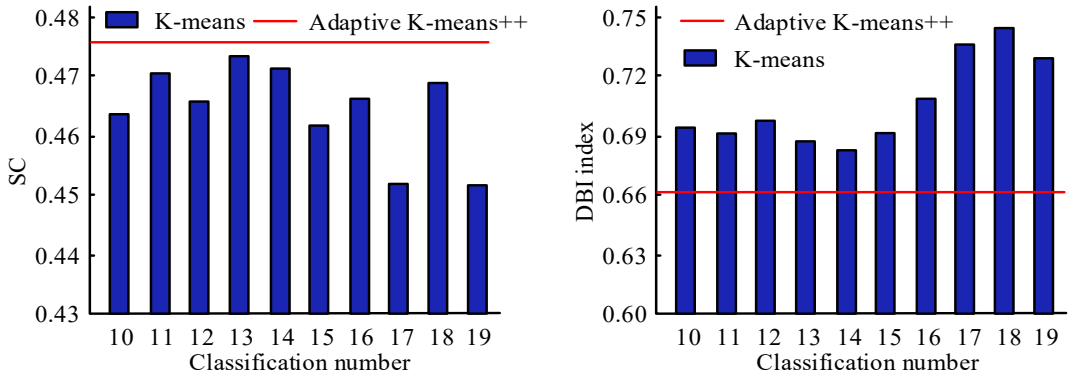

(a) The variation of the SC with the number of classifications N

(b) The variation of DBI with the number of classifications N

Fig. 7. Experimental analysis of the first layer clustering decomposition adaptive K-means++

Based on the demand for urban scheduling and management in an aging population, the number of nursing staff is determined by the total number of service demand points to be inspected in the area and the per capita inspection capacity μ. To balance human resource efficiency and inspection quality, the value of μ needs to be controlled within the range of 30 to 60. Too low will result in personnel redundancy, while too high will lead to insufficient inspection coverage. The WDM-KM algorithm was used to test 10 sets of parameters with μ values ranging from 30 to 60 and a step size of 5. The SC and DBI values were obtained, as shown in Fig. 8. The experimental results indicate that the DBI value and SC are optimal when μ is set to 35.

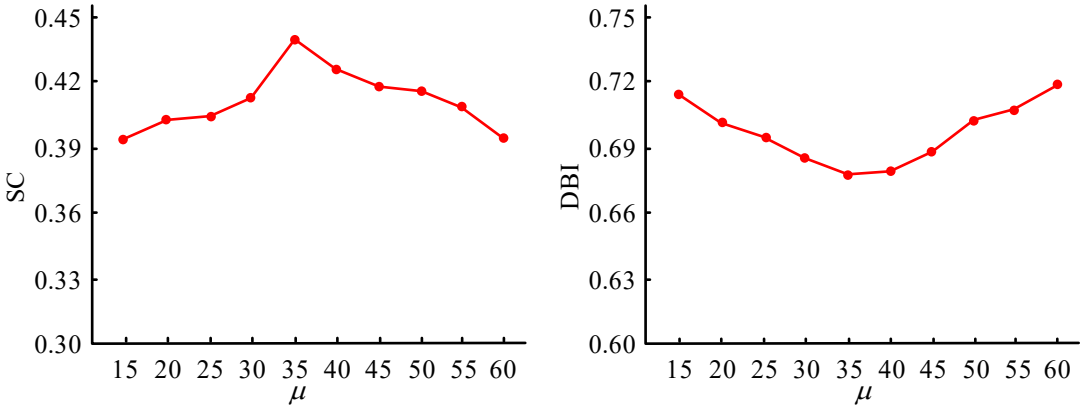

(a) The relationship between the number of issues to be inspected and the SC

(b) The relationship between the number of problems to be inspected and DBI

Fig. 8. Experimental Analysis of the second-level clustering decomposition

Fig. 9 shows the convergence of three algorithms during the iteration process. From Fig. 9 (a), in a 20×20 grid, the GA-ACO algorithm converged quickly in the first 20 iterations, with the shortest path length rapidly decreasing to 47.53 m, and remained stable in subsequent iterations. The traditional ACO algorithm exhibited significant fluctuations in the initial stage, and took a long time to converge. The final stable path length was still higher than that of GA-ACO. Although the algorithm in reference (Kooshari et al., 2024) has a faster convergence speed than traditional ACO, it still lags behind GA-ACO in terms of optimization accuracy and convergence efficiency. From Fig. 9 (b), in a 30×30 grid, the ACO algorithm, the algorithm in reference (Kooshari et al., 2024), and the GA-ACO algorithm discovered the current optimal path at the 91st, 46th, and 27th iterations, respectively. Compared to GA-ACO, the ACO algorithm and the algorithm in reference (Kooshari et al., 2024) required significantly more iterations to reach the optimal solution. This fully demonstrates that GA-ACO utilizes GA to generate initial pheromone distributions, effectively improving the convergence speed and solution quality of ant colony algorithms, and better meeting the efficiency requirements of service path planning in urban scheduling with aging populations.

Fig. 10 shows the path planning results of GA-ACO, GA, and ACO algorithms in 20×20 and 30×30 grid environments. As shown in Fig. 10 (a), in the 20×20 grid, the red path of GA-ACO had fewer turns and a more compact direction when bypassing obstacles. The blue path of GA had obvious detours, and the green path of ACO also generated redundancy due to local search limitations. As shown in Fig. 10 (b), a larger scale grid of 30×30, the red path of GA-ACO still maintained a more direct direction, effectively avoiding obstacles and having a shorter length, while the paths of GA and ACO exhibited more detours due to insufficient global search or limited local optimization. GA-ACO combines the global search capability of GA with the local optimization capability of ant colony algorithms to plan better service paths in obstacle environments of different scales, verifying its efficiency in complex spatial scheduling.

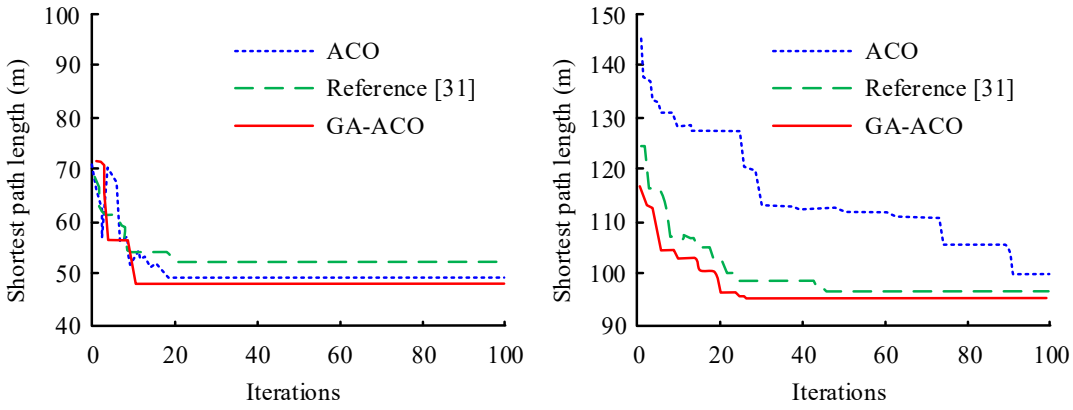

(a) The iterative convergence graphs of each algorithm in a 20×20 grid environment

(b) The iterative convergence graphs of each algorithm in a 30×30 grid environment

Fig. 9. The convergence curves of the GA-ACO algorithm and other algorithms

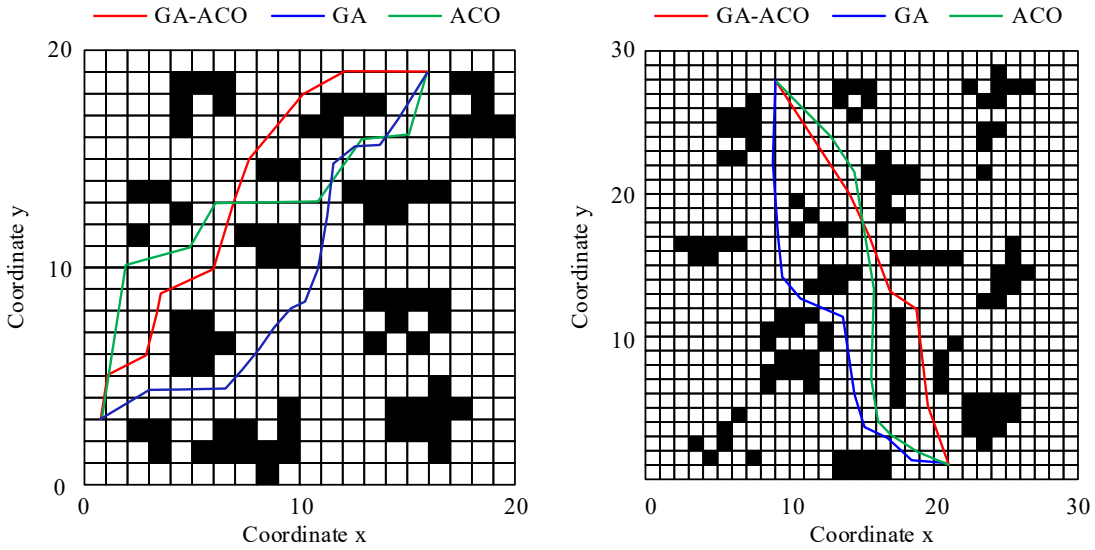

(a) 20×20

(b) 30×30

Fig. 10. Path planning results in the 20×20 grid and the 30×30 grid

Based on comparative experiments of four types of algorithms in a 20×20 grid scene, GA-ACO algorithm demonstrated comprehensive performance advantages. From Table 2, in terms of patrol efficiency, the average path length of 47.53 m was shortened by 18.0% compared to traditional ACO and improved by 5.8% compared to the algorithm in reference (Kooshari et al., 2024). The time cost of 68.7 minutes was the lowest in the entire game, which was 12.9% lower than that of the benchmark algorithm. The convergence performance of the algorithm was particularly outstanding, reaching a stable solution in only 20 iterations, which was 140% faster than ACO and 40% faster than reference (Kooshari et al., 2024). The stability index (path length standard deviation $\sigma = 0.85$) was significantly better than that of other algorithms, indicating its stronger anti-interference ability. Although the algorithm took 42.3 seconds to run, which was slightly higher than the reference (Kooshari et al., 2024), the patrol distance was reduced by 21.7% under the unit time cost, verifying the effectiveness of the hybrid architecture in balancing exploration and development mechanisms. The Particle Swarm Optimization (PSO) algorithm has strong group collaboration ability but is prone to premature convergence. Its path length was 13.2% longer than GA-ACO, and its stability was insufficient, indicating that it was difficult to handle complex spatial constraints. Although the path quality of the Simulated Annealing algorithm (SA) was close to GA-ACO (49.15 m), the time cost increased by 24.6% (85.6 min), and the single point iteration characteristic made it unable to adapt to real-time scheduling requirements. The hierarchical search mechanism in Grey Wolf Optimizer (GWO) algorithm improves convergence speed, but the linear position update strategy limits solution quality (path length +9.3%) and lacks robustness in dynamic obstacle environments. As a classic graph search algorithm, Dijkstra has a theoretical optimal path of 48.22 m, but global traversal leads to a significant increase in time consumption (135.7s), which cannot meet the timeliness requirements of large-scale scenarios.

Table 2. Comprehensive performance comparison of GA-ACO algorithm

Algorithm	Average Patrol Distance (m)	Scheduling Time Cost (min)	Convergence Iterations	Solution Stability	Algorithm Runtime (s)
GA-ACO	47.53	68.7	20	0.85	42.3
ACO	56.08	77.6	48	2.37	87.5
GA	52.41	72.9	35	1.92	63.8
Reference (Kooshari et al. 2024)	50.27	70.5	28	1.45	58.6
PSO	53.82	75.3	32	1.78	71.2
SA	49.15	85.6	/	1.05	102.4
GWO	51.94	73.8	29	1.63	67.9
Dijkstra	48.22	94.2	/	0.92	135.7

3.2. Practical Case Application: Scheduling of Elderly Community Medical Services in Shanghai

To further verify the practicality and robustness of the algorithm in real urban environments, this study takes the scheduling of elderly community medical services in Shanghai as a practical application case, using the road network data extracted from OpenStreetMap at the district level in Shanghai, to explore its responsiveness and resource optimization effect on the service needs of the elderly population under real spatiotemporal constraints. Based on the demand for urban scheduling management in an aging population, after optimizing the parameters of the two-layer clustering, typical law enforcement areas are selected to demonstrate the decomposition effect. Fig. 11 (a) presents the subset partitioning results of the WDM-KM algorithm on the problem dataset, while Fig. 11 (b) displays the clustering geographic distribution in conjunction with the spatial location of law service base stations. As shown in Fig. 11, after the second layer clustering processing, all service demand points within the law enforcement area are decoupled into several independent sub-problem sets, significantly reducing the scale of subsequent path planning solutions and transforming the multi-nursing staff collaborative path problem into a single nursing staff path optimization problem, and effectively reducing the complexity of GA-ACO.

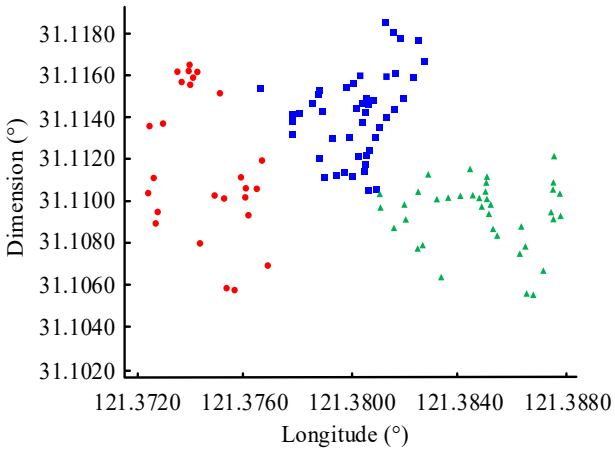

(a) Classification results

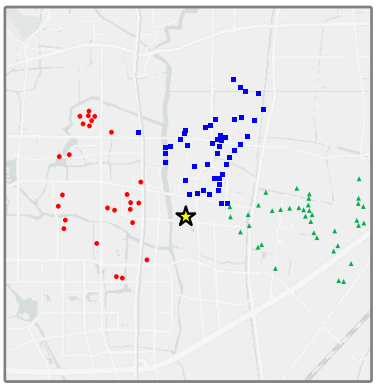

(b) Project the classification results and the locations of law enforcement points on the map

Fig. 11. Clustering results

The GA-ACO algorithm path planning results in aging cities are shown in Fig. 12, which displays the closed-loop patrol routes of multiple nursing staff through spatial coordinate mapping. As shown in Fig. 12, the nursing staff started from the central law service base station, performed patrol tasks along the sequence of service demand points indicated by latitude and longitude coordinates, and finally returned to the starting point. The visualization results validate the effectiveness of the improved ant colony algorithm on the decomposed sub-problem set, forming an optimized path without crossover and full coverage, while providing spatial decision support for efficient patrol in densely populated areas.

Table 3 shows the implementation effect of the proposed population aging urban scheduling management algorithm in key areas such as Jing'an, Huangpu, Chongming, and Jinshan in Shanghai. Furthermore, the average response time in each region decreased from 20.3-35.7 minutes to 15.2-26.7 minutes, with an overall reduction of 25%. Jing'an District reduced from 22.5 minutes to 16.8 minutes, reflecting the rapid response optimization capability under high-density demand in the central area. The resource coverage efficiency increased from 55.3%-71.5% to 77.6%-93.8%, with an overall increase of 30%. Chongming District, as a suburban area, had a 40.3% increase in coverage efficiency, verifying the algorithm adaptability to different geographical environments. The standard deviation of personnel load decreased from 17.9-22.4 to 10.8-13.5, and the overall coefficient of variation decreased from 0.32 to 0.19, indicating a significant improvement in task allocation balance. From overall indicators, the algorithm achieves a synergistic improvement in response time, coverage efficiency, and load balance through adaptive K-means++ dynamic layout of law service base stations, combined with WDM-KM's fine task allocation and GA-ACO's path optimization. Especially in resource sparse areas such as Chongming District, the improvement is greater, proving that the algorithm can effectively optimize scheduling management in different scenarios of aging cities and provide data support for precise medical resource allocation.

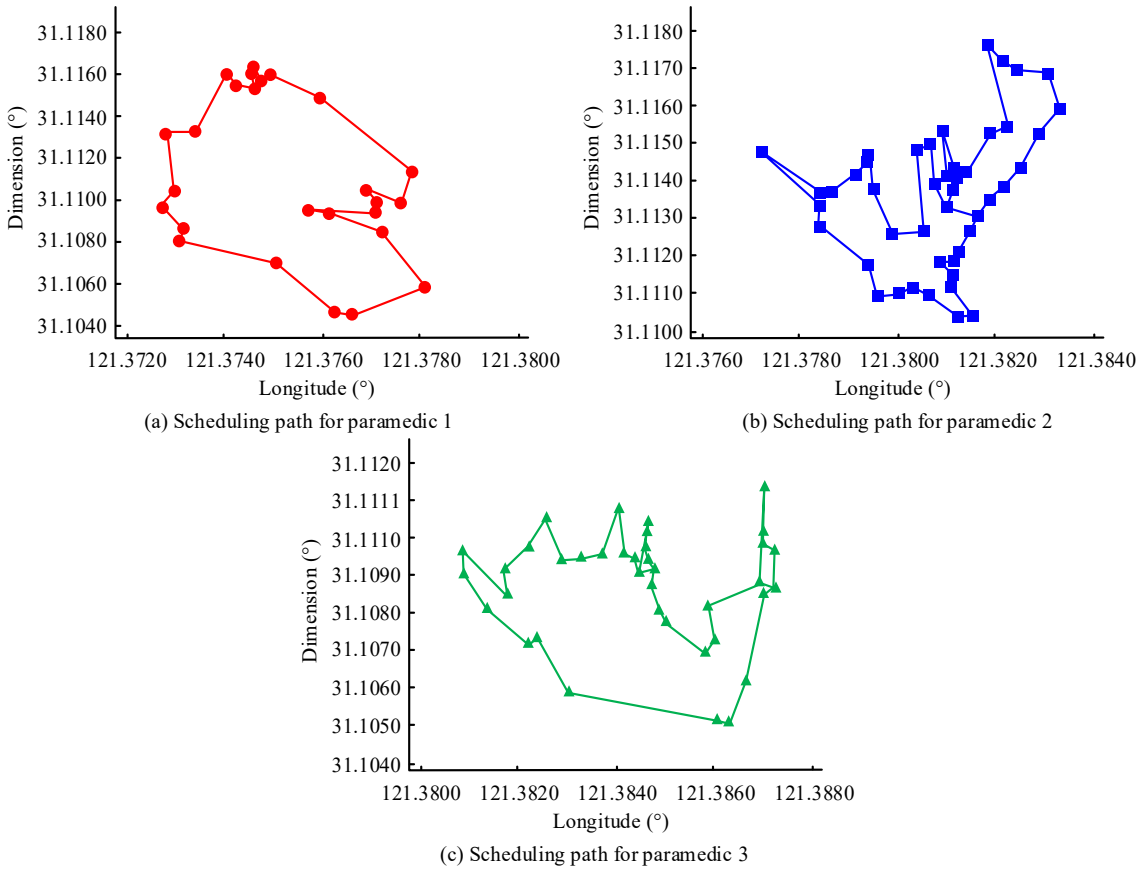

Fig. 12. Path planning results of different clustering results

Table 3. Implementation effect of scheduling

Domain	Indicator	Before application	After application	Increase the proportion
Jing'an District	Average Response Time (min)	22.5	16.8	0.253
	Resource coverage efficiency (%)	68.2	92.4	0.355
	Standard deviation of personnel load	18.6	11.2	0.409
Huangpu District	Average Response Time (min)	20.3	15.2	0.251
	Resource coverage efficiency (%)	71.5	93.8	0.312
	Standard deviation of personnel load	17.9	10.8	0.397
Chongming District	Average response time (minutes)	35.7	26.7	0.252
	Resource coverage efficiency (%)	55.3	77.6	0.403
	Standard deviation of personnel load	22.4	13.5	0.397
Jinshan District	Average Response Time (min)	28.4	21.3	0.25
	Resource coverage efficiency (%)	62.1	84.7	0.364
	Standard deviation of personnel load	19.8	12.1	0.389
Overall	Average Response Time (min)	26.7	20	0.25
	Resource coverage efficiency (%)	64.2	83.5	0.3
	Personnel load balance degree (coefficient of variation)	0.32	0.19	0.406

4. Discussion

The urban scheduling management framework integrates clustering decomposition with an improved hybrid ant colony algorithm, demonstrating significant advantages in addressing the resource scheduling challenges in aging populations. In terms of algorithm performance, the adaptive K-means++ algorithm achieved an SC to 0.475 through a dynamic weighting mechanism, significantly optimizing intra-class cohesion and inter-class separation compared to the traditional K-means algorithm. This improvement stems directly from coupling demand intensity with spatial accessibility, enabling service station layouts that better match the spatiotemporal aggregation patterns of the elderly population. The WDM-KM algorithm further achieves task balance allocation through a walking distance matrix. When the per capita patrol ability was set to 35, the DBI value dropped to 0.661, verifying the promoting effect of the clustering strategy based on actual travel constraints on personnel load balance.

In path optimization, the GA-ACO hybrid algorithm used GA-generated initial pheromone distributions to reduce the average path length in a 30×30 grid scenario to 47.53m, which was 18.0% higher than the traditional ACO. Convergence

iteration times were reduced from 48 to 20, demonstrating the synergistic effect of global search and local optimization. This advantage is translated into practical applications in Shanghai's aging communities, resulting in an average response time reduction of 25% and a 30% increase in resource coverage efficiency. Especially in resource sparse areas such as Chongming District, the coverage efficiency was improved by 40.3%, demonstrating the adaptability of the algorithm to different geographical environments.

Compared to existing research, the two-layer clustering model overcomes limitations of traditional static layout by transforming the spatiotemporal aging demand characteristics into computable scheduling parameters via adaptive weighting and dynamic constraint. The improved ant colony algorithm introduces genetic operations and adaptive volatility mechanism, effectively preventing traditional local optima traps in multi-constraint scenarios. Additionally, while the research has limitations: Firstly, the model does not integrate real-time traffic data, and the static walking distance matrix it relies on may have biases in dynamic scenarios such as traffic congestion; Secondly, although the algorithm parameters (such as the adaptive weight coefficient) have been experimentally calibrated, their versatility under different urban scales requires further verification. In the future, a real-time demand prediction module can be introduced, combined with deep learning models to capture the dynamic changes in aging service demand. By integrating traffic flow data to optimize walking distance calculation, the timeliness of path planning can be improved.

5. Conclusion

This study proposed an integrated scheduling management framework that combined clustering decomposition and an improved hybrid ant colony algorithm to address the spatiotemporal supply-demand contradiction in urban resource scheduling for aging populations. By constructing a two-layer clustering model using an adaptive K-means++ algorithm to optimize base station layout, and WDM-KM algorithm to achieve balanced task allocation, combined with a GA-enhanced ACO strategy, the management of law enforcement stations, personnel allocation, and intelligent path optimization. Experimental results demonstrated that the framework outperformed traditional algorithms in both clustering quality and path optimization efficiency in 20×20 and 30×30 grid scenarios. In the medical service scheduling in aging communities in Shanghai, the average response time was reduced by 25%, the resource coverage efficiency was improved by 30%, and the standard deviation of personnel load was reduced by more than 40%. The results provide a quantitative decision-making tool for precise resource allocation. The core value of this research lies in integrating data mining, swarm intelligence, and social science models, effectively addressing the challenges of spatiotemporal clustering and dynamic fluctuations in aging-related demand.

Author Contributions

Fei Pang contributes to draft preparation, manuscript editing and funding acquisition. Yingxu Li contributes to methodology, analysis, manuscript editing, and funding acquisition. Guo Miao contributes to data collection, conceptualization. Yun Shi contributes to software, manuscript review.

Funding

The research is supported by: (Research on the positive interaction mechanism between education supply and population fertility, (No.21YJC840017), Fei Pang and Yingxu Li are co-authors; School Mentor Support Program: “Research on the Positive Interaction Mechanism between Educational Resource Allocation and Population Fertility” (XDW2025101); School Mentor Support Program: “Research on the Mechanism and Path of China's Global Value Chain climbing under the RCEP Framework” (XDW2025102).

Institutional Review Board Statement

Not applicable.

Reference

Bai, R., Shi, Y., Yue, M., and Du, X. (2023). Hybrid model based on K-means++ algorithm, optimal similar day approach, and long short-term memory neural network for short-term photovoltaic power prediction. *Global Energy Interconnection*, 6(2), 184-196. doi: 10.1016/j.gloei.2023.04.006

Chen, J., Song, W., Zuo, X., Zhao, K., Jin, B., Zhu, D., and Dai, B. (2024). 1DCAE-TSSAMC: Two-Stage Multi-Dimensional Spatial Features Based Multi-View Deep Clustering for Time Series Data. *International Journal of Uncertainty, Fuzziness and Knowledge-Based Systems*, 32(4), 593-623. doi: 10.1142/S0218488524400105

Chen, W., Liu, X., Chen, X., Cheng, L., and Chen, J. (2025). Deciphering flow clusters from large-scale free-floating bike sharing journey data: a two-stage flow clustering method. *Transportation*, 52(1), 155–184. doi: 10.1007/s11116-023-10415-y

Chowdhury, A. R., Hazra, J., Dasgupta, K., and Dutta, P. (2024). Fuzzy rule-based hyperspectral band selection algorithm with ant colony optimization. *Innovations in Systems and Software Engineering*, 20(2), 161-174. doi: 10.1007/s11334-021-00432-4

Dural Selcuk, G. and Vasilakis, C. (2023). Evaluating the sustainability of complex health system transformation in the context of population ageing: An empirical system dynamics study. *Journal of the Operational Research Society*, 74(1), 1-17. doi: 10.1080/01605682.2021.1992307

Fan, L. (2024). A two-stage hybrid ant colony algorithm for multi-depot half-open time-dependent electric vehicle routing problem. *Complex & Intelligent Systems*, 10(2), 2107-2128. doi: 10.1007/s40747-023-01259-1

Gao, B., Zhu, Y., and Li, Y. (2023). Optimal operation strategy analysis with scenario generation method based on principal component analysis, density canopy, and k-medoids for integrated energy systems. *Journal of Modern Power Systems and Clean Energy*, 12(1), 89-100. doi: 10.35833/MPCE.2022.000681

He, J., Teng, Z., and Zhang, F. (2024). Research on Power Control Routing Algorithm for Wireless Sensor Networks Based on Ant Colony Optimization. *Wireless Personal Communications*, 137(2), 1119-1139. doi: 10.1007/s11277-024-11455-y

Jasim, Z. K. J. and Kurnaz, S. (2024). An improved image steganography security and capacity using ant colony algorithm optimization. *Computers, Materials & Continua*, 80(9), 4643-4662. doi: 10.32604/cmc.2024.055195

Klose, A., Wagner-Stürz, D., Neuendorf, L., Oeing, J., Khaydarov, V., and Schleehahn, M. (2023). Automated evaluation of biochemical plant KPIs based on DEXPI information. *Chemie Ingenieur Technik*, 95(7), 1165-1171. doi: 10.1002/cite.202200239

Kooshari, A., Fartash, M., Mihannezhad, P., Chahardoli, M., AkbariTorkestani, J., and Nazari, S. (2024). An optimization method in wireless sensor network routing and IoT with water strider algorithm and ant colony optimization algorithm. *Evolving Systems*, 17(3), 1527-1545. doi: 10.1007/s12065-023-00847-x

Li, W., Yan, X., and Huang, Y. (2024). Cooperative-guided ant colony optimization with knowledge learning for job shop scheduling problem. *Tsinghua Science and Technology*, 29(5), 1283-1299. doi: 10.26599/TST.2023.9010098

Li, X., Wang, D., Tian, Y., and Kong, X. (2023). A method for extracting interference striations in lofargram based on decomposition and clustering. *IET Image Processing*, 17(6), 1951-1958. doi: 10.1049/ipr2.12768

Moghadam, P. and Ahmadi, A. (2024). A novel two-stage bio-inspired method using red deer algorithm for data clustering. *Evolving Systems*, 17(3), 1819-1836. doi: 10.1007/s12065-023-00864-w

Mpia, H. N., Syasimwa, L. M., and Muyisa, D. M. (2025). Comparative machine learning models for predicting loan fructification in a semi-urban area. *Archives of Advanced Engineering Science*, 3(2), 124-134. doi: 10.47852/bonviewAAES42022418

Mulo, T., Syam, P., and Choudhury, A. B. (2023). Hybrid and modified harmony search optimization application in economic load dispatch with integrated renewable source. *Electrical Engineering*, 105(3), 1923-1935. doi: 10.1007/s00202-023-01770-1

Ranjbar Noshari, N., Azgomi, H., and Asghari, A. (2024). Efficient clustering in data mining applications based on harmony search and k-medoids. *Soft Computing*, 28(23), 13245-13268. doi: 10.1007/s00500-024-10337-6

Saranya, V. G. and Karthik, S. (2024). Bio-inspired intelligent routing in WSN: Integrating mayfly optimization and enhanced ant colony optimization for energy-efficient cluster formation and maintenance. *Computer Modeling in Engineering & Sciences*, 141(10), 127-150. doi: 10.32604/cmes.2024.053825

Sarker, M. A. A., Asgari, H., and Jin, X. (2023). Aging population and automated mobility: exploring the impacts of land use patterns and attitudes. *Transportation Research Record*, 2677(10), 136-152. doi: 10.1177/03611981231160548

Shou, M., Jia, F., and Yu, J. (2024). Developing urban infrastructure constructions for increasing e-commerce sales: the moderating roles of aging population. *Industrial Management & Data Systems*, 124(5), 1971-1990. doi: 10.1108/IMDS-03-2023-0175

Stodola, P. and Nohel, J. (2022). Adaptive ant colony optimization with node clustering for the multidepot vehicle routing problem. *IEEE Transactions on Evolutionary Computation*, 27(6), 1866-1880. doi: 10.1109/TEVC.2022.3230042

Tanimu, J., Shiaeles, S., and Adda, M. (2024). A comparative analysis of feature eliminator methods to improve machine learning phishing detection. *Journal of Data Science and Intelligent Systems*, 2(2), 87-99. doi: 10.47852/bonviewJDSIS32021736

Theodorou, P. and Christopoulos, D. T. (2024). Electricity demand, forecasting the peaks: development and implementation of C-EVA method. *Green and Low-Carbon Economy*, 2(4), 310-324. doi: 10.47852/bonviewGLCE42022327

Wang, H., Yang, X., Meng, L., Yin, X., Wang, Z., Wang, Z., and Wang, Y. (2025). Transportation Route Optimization of Municipal Solid Waste Based on Improved Ant Colony Algorithm in Internet of Vehicles. *IEEE Transactions on Vehicular Technology*, 74(2), 2129−2142. doi: 10.1109/TVT.2024.3417976

Wenya, W. Z. and Ze, F. (2025). Biotechnology commercial exploration: cross-border e-commerce logistics distribution based on multi-objective optimization. *Journal of Commercial Biotechnology*, 30(1), 172-184. doi: 10.5912/jcb2496

Wu, B., Zuo, X., Zhou, M., Wan, X., Zhao, X., and Yang, S. (2024). A multi-objective ant colony system-based approach to transit route network adjustment. *IEEE Transactions on Intelligent Transportation Systems*, 25(7), 7878-7892. doi: 10.1109/TITS.2023.3348111

Xu, B., Wu, D., Shi, J., Cong, J., Lu, M., Yang, F., and Nener, B. (2024). Isolated random forest assisted spatio-temporal ant colony evolutionary algorithm for cell tracking in time-lapse sequences. *IEEE Journal of Biomedical and Health Informatics*, 28(7), 4157-4169. doi: 10.1109/JBHI.2024.3393493

Yastrebov, A., Kubuś, Ł., and Poczeta, K. (2023). Multiobjective evolutionary algorithm IDEA and k-means clustering for modeling multidimenional medical data based on fuzzy cognitive maps. *Natural Computing*, 22(3), 601-611. doi: 10.1007/s11047-022-09895-1

Yu, H. (2024). The impact of path planning model based on improved ant colony optimization algorithm on green traffic management. *International Journal of Advanced Computer Science and Applications*, 15(6), 1065−1074. doi: 10.14569/ijacsa.2024.01506109

Zhang, H., Cao, J., Liang, H., and Cheng, G. (2024). Research on corrosion defect identification and risk assessment of well control equipment based on a machine learning algorithm. *Petroleum*, 10(4), 736-744. doi: 10.1016/j.petlm.2022.07.003

Zheng, L., Qu, X., and Li, J. (2023). distributed iterative node localization via an advanced K-Means++ procedure in WSNs. *IEEE Sensors Journal*, 23(22), 27500-27507. doi: 10.1109/JSEN.2023.3315300

Fei Pang is currently an Associate Professor in the School of Education Science, Hanshan Normal University, Chaozhou 52041, China. He received Ph.D. in Sociology with research interests in education and population issues, social welfare and social work, including social psychology.

Yingxu Li is an Associate Professor in the College of Economics and Management at Hanshan Normal University, Guangdong Province, China. She obtained her Ph.D. in World Economics in 2012 from the School of Economics at Jilin University. She serves on the Teaching Steering Committee for Economics and Trade Majors in Undergraduate Institutions of Guangdong Province and is a council member of the Guangdong Society of World Economics. Her work has been published in over 30 domestic and international academic journals and conference proceedings. Her research interests include the world economy, the educational economy, and the industrial economy.

Guo Miao, PhD in Sociology, is an Associate Researcher at the Regional Modernization Institute, Jiangsu Academy of Social Sciences, Nanjing 210046. He is a recipient of the Jiangsu "Purple Gold Cultural and Social Science Outstanding Youth" award, a Master's Supervisor, Senior Visiting Scholar at the School of Population and Health, Renmin University of China. He currently serves as Vice Chairman of the Population and Policy Special Committee of the China Population Society and is a member of the Silver Hair Economy Special Committee of the China Labor Economics Society.

Yun Shi is a Lecturer at the School of Education Science, Hanshan Normal University, Chaozhou 52041, China. She has a Doctor of Philosophy in Education from SEGi University, Malaysia. Her research interests include preschool education, primary school education, and teacher education.